

Nanostructured doped zinc oxide thin solid films: the effect of different doping elements on the electrical and morphological properties

Dwight R. Acosta^a, A. Guillén-Santiago^a, L. Castañeda^b, A. Maldonado^c and M. de la L. Olvera^{c,*}

^aInstituto de Física, Universidad Nacional Autónoma de México, IFUNAM, Apartado Postal 20-364, México, D.F., 01000, México.

^bInstituto de Física, Universidad Autónoma de Puebla, Apartado Postal J-48, Puebla 72570, México.

^cDepartamento de Ingeniería Eléctrica, Centro de Investigación y de Estudios Avanzados del Instituto Politécnico Nacional CINVESTAV-IPN, SEES, Apartado Postal 14740, México, D.F., 07000, México.

Zinc oxide (ZnO) is a multifunctional semiconductor with a wide direct band gap (3.3 eV); due to its tunable optoelectronic characteristics it is one of the transparent conductive oxides (TCO) materials most commonly used as front and back transparent conductors in photovoltaic cells (PVC) architecture. The electrical and optical properties of TCO materials strongly depend on the crystalline defects (oxygen vacancies/interstitial zinc) and on the nature, as well on the amount of foreign atoms trapped in the host lattice. In this study a summary of some results of ZnO thin solid films deposited by the pneumatic spray pyrolysis technique, and doped with several different atoms, namely, Fluorine (F), Gallium (Ga) and Indium (In), are given. The materials synthesis was carried out for each doped ZnO film with a systematic variation in: substrate temperature, and doping concentration of the starting solutions. The influence of the variations of these deposition parameters on the electrical and structural properties of the ZnO films synthesized is presented and discussed.

Key words: zinc oxide, chemical spray, thin films.

Introduction

The so-called eco-materials are directly related to the improvement of energy production, energy saving and environmental protection. Zinc oxide (ZnO), is a multifunctional “*n-type*” wide band gap AII-BVI semiconductor with an hexagonal wurtzite crystalline structure, which is commonly used in the items just mentioned, and in a thin solid film design is of great interest due to the wide variety of applications in different optoelectronic devices [1-3]. Moreover, the simultaneous concurrence of high transparency in the visible region (> 90%), refractive index values (ranging from 1.7 to 2), and lower resistivity (ranging from 10^{-3} to 10^{-4} Ω cm) enable this to act as an effective antireflection coating, transparent conductive electrode, window layer in solar cells [4], as well as a light-emitting device [5]. Other ZnO physical properties give rise to different applications, as is the case in heat mirrors [6], gas sensors [7], and acoustic wave filters [8]. ZnO thin solid films deposited by the chemical spray technique (CST) compete well with thin films deposited by physical techniques. In addition, the CST is based on a simple and economical equipment and it is also useful for large-area applications. Despite the large number of reports on chemically sprayed ZnO thin films, it is still not clear what physical phenomena

limit their electrical conductivity. In this respect, in spite of the fact that the transport mechanisms in ZnO thin films are strongly correlated with specific types of intrinsic structural defects, it is not clear how other point or linear defects, stacking faults and grain boundaries affect the electrical properties.

The intentional and selective addition of impurities into the ZnO lattice, in order to decrease the electrical resistivity, induces drastic changes in the transport, morphological, structural, and optical properties of the deposited films. The performance of the dopant element depends on its nature, such as the electronegativity and ionic radius. In the case of using higher valence elements, named cationic impurities (Aluminum (Al), Boron (B), Gallium (Ga), Indium (In)) in ZnO, it is believed that the effective doping is achieved when Zn^{2+} ions are replaced by the impurities; whereas, in lower valence elements are used as dopants, as is the case of Fluorine (F), named anionic impurities, it is supposed that the oxygen ions are replaced by the impurities. The effect of different dopant elements such as Aluminum (Al), Cobalt (Co), Copper (Cu), Indium (In), Iron (Fe), and Tin (Sn) on the microstructure of ZnO thin films has also been investigated in detail [7, 9]. This study aims at comparing the electrical and morphological behaviors of ZnO films doped with Ga as well as In like cationic impurities and F as anionic impurity.

Experimental Procedure

All the thin solid films were deposited on sodocalcic glass substrates, carefully cleaned prior to the deposition. The

*Corresponding author:
Tel : +52-55-5747-3784
Fax: +52-55-5747 3978
E-mail: molvera@cinvestav.mx

detailed deposition parameters and synthesis conditions have been previously reported: Indium-doped Zinc Oxide (ZnO : In) [10], Gallium-doped Zinc Oxide (ZnO : Ga) [11], and Fluorine-doped Zinc Oxide (ZnO : F) [12, 13]. In order to compare the influence of different doping atoms, we have chosen the results for films deposited under quite similar conditions (0.2 M). The deposition procedure for all the cases was as follows: the substrates were heated on a fused tin bath, whose temperature is measured just below the substrate using a thin chromel-alumel thermocouple contained in a stainless steel metal jacket. The substrate temperature (T_s) was ranged from 425 to 500 °C in steps of 25 °C. The solution and Nitrogen (N_2) gas flows employed in this work were 12 ml min^{-1} and 8 L min^{-1} , respectively. The sheet resistance was measured in darkness at room temperature using the conventional four-aligned probes method in a Veeco FPP100 equipment. The electrical resistivity, ρ , was calculated by the relation $\rho = R_s \cdot d$, where R_s is the sheet resistance and d is the film thickness. For the electron microscopy studies the deposited films were stripped off carefully following standard procedures and the observations were carried out in a FEG 2010F JEOL microscope. Scanning electron microscopy observations were carried out in a JEOL 5600 LV microscope in order to determine morphological and topological details of our samples.

Results and Discussion

Electrical properties

ZnO : In

The variation in the resistivity of the ZnO : In thin films as a function of both the [In]/[Zn] ratio in the solution and the substrate temperature (T_s) is shown in Fig. 1. It is evident that for a fixed T_s , as the In concentration in the solution increases, the resistivity of the ZnO : In thin films decreases, reaching a minimum value depending on the T_s . Further increase in the [In]/[Zn] value in the solution leads to an increase in the resistivity values of the ZnO : In thin films. Concerning the effect of the substrate temperature, a similar trend is observed: the resistivity of the ZnO : In thin films decreases with increasing T_s , again reaching a minimum value, and then it increases with a further increase in the T_s values. The lowest resistivity value is of the order of $4.1 \times 10^3 \Omega \text{ cm}$ for ZnO : In thin films deposited with a dopant content of [In]/[Zn] = 6 at.%, within the 450-475 °C interval.

ZnO : Ga

In Fig. 2, for ZnO : Ga thin solid films, it can be observed that the electrical resistivity decreases as the substrate temperature increases, until a minimum resistivity value is reached. This result is associated with a improved film formation; beyond this optimal temperature the film resistivity increases due to both the zinc oxide formation with a better stoichiometry (a highly resistivity phase) and the out-diffusion of alkaline ions, Potassium (K), Calcium

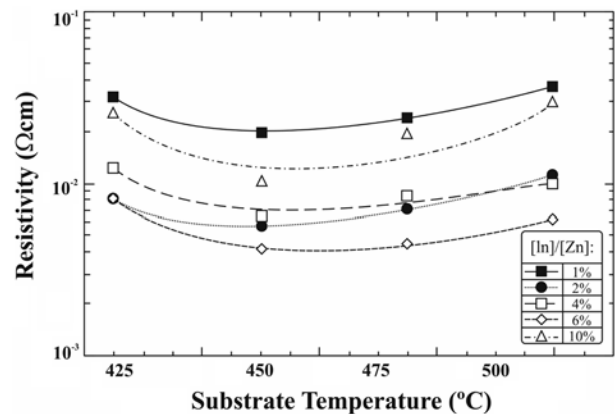


Fig. 1. Electrical resistivity as a function of the [In]/[Zn] concentration in the starting solution, for ZnO : In films deposited at different substrate temperatures.

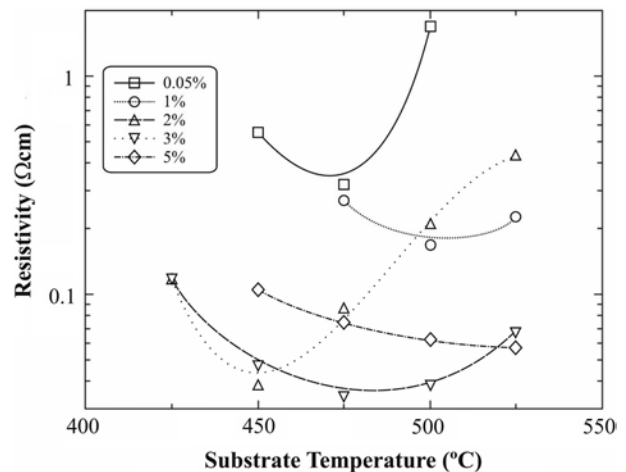


Fig. 2. Variation of the electrical resistivity with the substrate temperature for as-deposited ZnO : Ga films at different [Ga]/[Zn] (at.%) ratios.

(Ca), Sodium (Na), and Silicon (Si) coming from the glass substrate into the film, which compensate the free electrons. The electrical resistivity as a function of the [Ga]/[Zn] ratio in the starting solution shows a decrease as the [Ga]/[Zn] rate is increased, reaching a minimum value at a certain [Ga]/[Zn] ratio (2-3 at.%), further increase in the resistivity values is observed when the [Ga]/[Zn] ratio increases. For low [Ga]/[Zn] ratios the resistivity decrease is due to the increase of the Ga atoms that are incorporated into the lattice ZnO in the Zn sites, supplying one electron to the conduction band for each Ga atom, until the maximum solubility of Ga into the ZnO lattice is reached (minimum value of the resistivity curve).

ZnO : F

In Fig. 3, ZnO : F thin films show high resistivity values when these are deposited from a fresh solution. The resistivity values are usually in the range from 1 to $0.01 \Omega \text{ cm}$. However, when the solution was aged for at least three days, the resistivity decreases, as a value of the order of

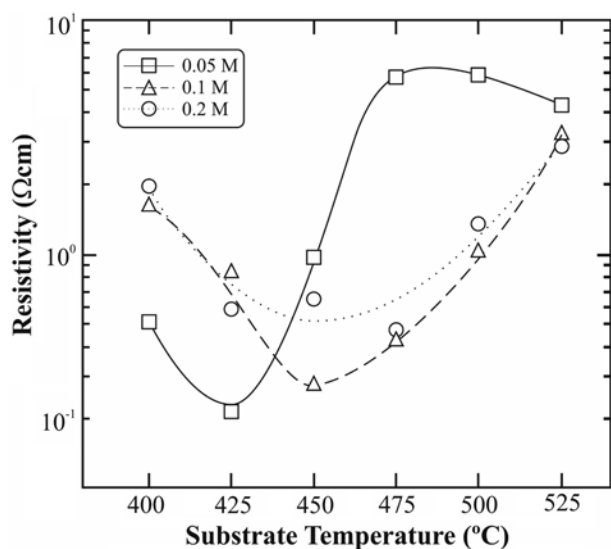


Fig. 3. Electrical resistivity as a function of substrate temperature for ZnO : F thin films obtained from a fresh solution at different molarities and the optimal [F]/[Zn] ratio for each case.

$6.7 \times 10^{-3} \Omega \text{ cm}$ was obtained [13]. The variation of the electrical resistivity with the substrate temperature follows a similar trend observed with a cationic impurity. In fact, for low substrate temperatures, the resistivity is high, due to incomplete synthesis of ZnO; as the substrate temperature is increased, the resistivity of the films decreases reaching a minimum, due to an optimal stoichiometric deviation; further increase in the substrate temperature results in an increase in the corresponding resistivity of the films, due to the same reasons given above for cationic impurities. The ZnO : In thin films doped with cationic elements, namely In and Ga, show noticeable variations in the electrical characteristics. In fact, the minimal electrical resistivity of as-grown ZnO : In and ZnO : Ga thin films were $4.1 \times 10^{-3} \Omega \text{ cm}$ and $3.6 \times 10^{-2} \Omega \text{ cm}$, respectively. In the last case, an annealing treatment in vacuum leads to a decrease of the resistivity to the order of $8 \times 10^{-3} \Omega \text{ cm}$. The effect of the substrate temperature on the electrical resistivity of ZnO : Ga thin films agrees well with that reported by other authors, although in the case of the ZnO : In films, the effect is less significant [13].

Morphological and structural studies

ZnO : In

In Fig. 4a, the surface morphology of a ZnO : In thin film is illustrated and the grains present a randomly oriented flake-like configuration with at least two different grain sizes. An intergranular space is visible along the sample and contributes to variations in the surface roughness. In Fig. 4b, a high resolution electron microscopy (HREM) micrograph reveals the presence of a polycrystalline nanostructured material with grains in different crystallographic orientations.

ZnO : Ga

In Fig. 5a a SEM micrograph shows the surface of a

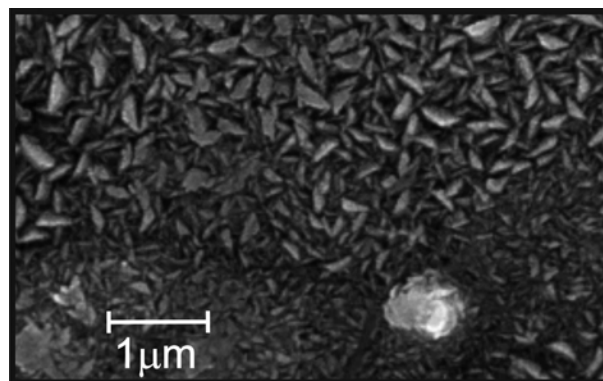


Fig. 4a. ZnO:In thin film deposited at 475 °C with a [In]/[Zn] = 6 at.% concentration in the starting solution. Two different sizes for flake-like grains can be observed.

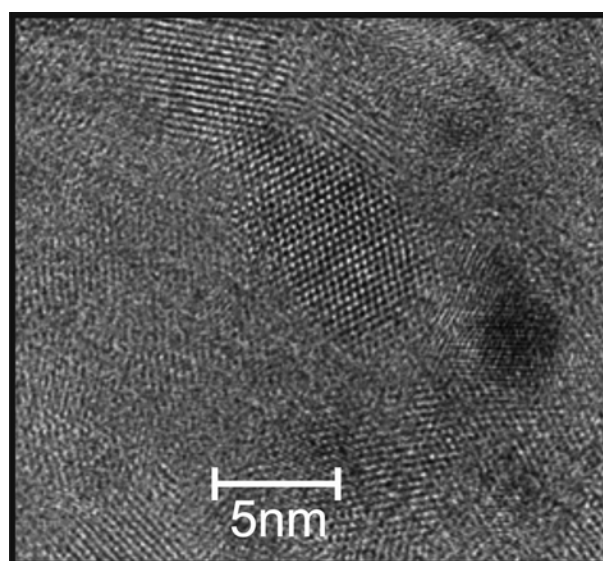


Fig. 4b. HREM micrograph of the ZnO:In thin film displayed in Fig. 4a. Amorphous-like zones and grains with different orientation and sizes of can be seen.

ZnO : Ga film deposited with a [Ga]/[Zn] = 0.05 at. % ratio, and deposited at $T_s = 475 \text{ °C}$. This micrograph shows a regular surface morphology formed of small and large rounded grains with sizes running from 110 to 260 nm. The 5a and 5b images suggest a film with a low roughness and porosity. The HREM micrograph displayed in Fig. 5b shows ZnO : Ga grains in different orientations with not well defined grain boundaries among them.

ZnO : F

Fig. 6a presents a SEM micrograph of a ZnO : F thin film. The showed morphology gives the impression of being a regular with apparently rounded primary grains with sizes ranging from 100 to 220 nm as well as secondary grains. Under appropriate deposition conditions, the chemical spray technique let us produce a nanomaterial with specific structural and physical properties, which can compete well with films produced by physical techniques. In the case of the ZnO : F thin films, the surface is one typical of chemically

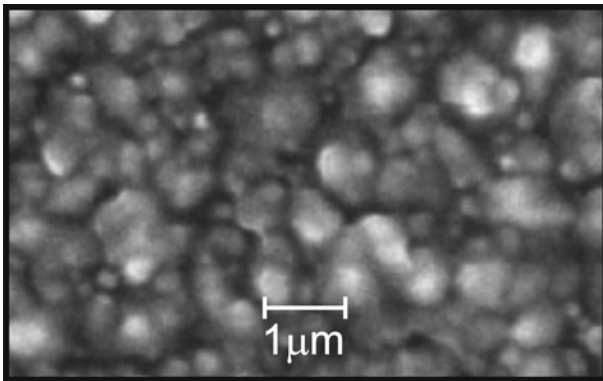


Fig. 5a. SEM micrograph from a ZnO : Ga film deposited at $T_s = 475^\circ\text{C}$ from a 0.2 M starting solution. A regular surface with two grains sizes of rounded grains is observed.

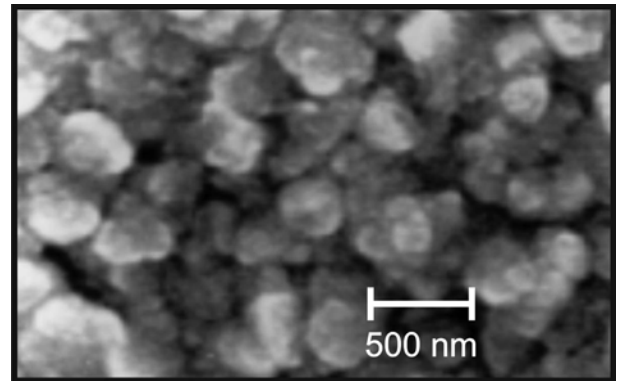


Fig. 6a. SEM image of a ZnO : F film with $T_s = 450^\circ\text{C}$ and 0.2 M in solution and $[\text{F}]/[\text{Zn}] = 50$ at.%. The grain surfaces seem rough with inter grain pores along the film surface.

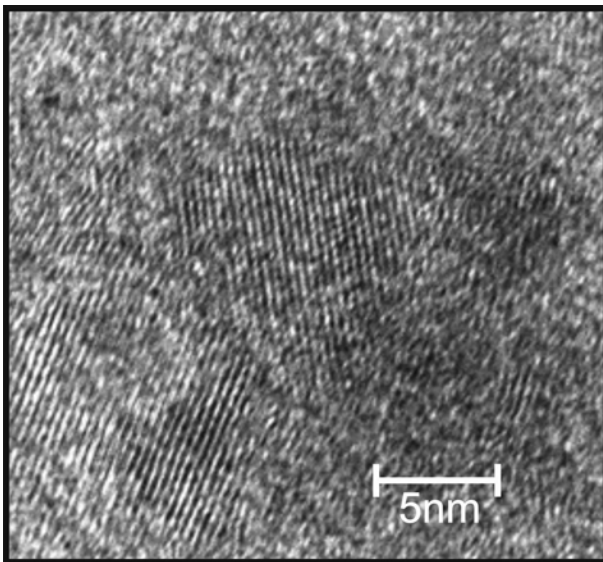


Fig. 5b. HREM micrograph showing the structure of one of the large grains observed in Fig. 5a.

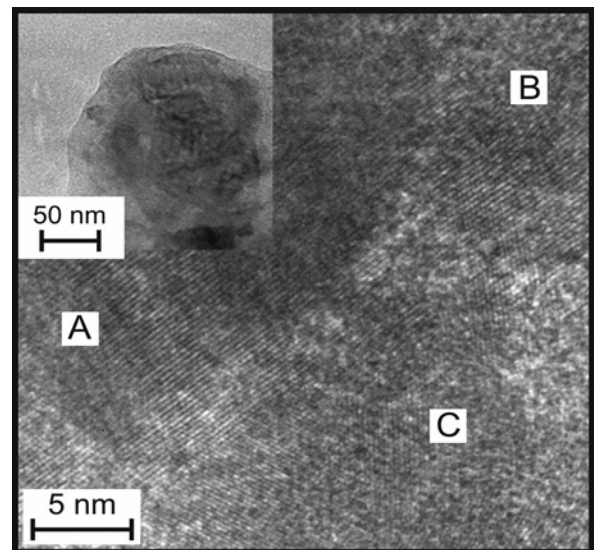


Fig. 6b. HREM micrograph coming from the ZnO : F film presented in the inset (upper left). The film looks uniform and continuous. The grains labeled A, B and C show different crystallographic orientations.

sprayed films, since rounded grains are observed. When the film thickness is varied, a general trend observed in the ZnO thin films is the agglomeration of grains to form secondary grains, which in turn might lead to a decrease of grain boundary charge scattering.

From electron microscopy images and electron and X-ray diffraction studies (not reported here), all the films are polycrystalline in character, fitting well with the hexagonal wurtzite type ZnO. Irrespective of the deposition conditions, the ZnO : F and ZnO : Ga thin films all show (002) preferential growth. In contrast the ZnO : In thin films show the (101) planes that prevail or at least contribute in a significant way depending on the deposition conditions. In the literature there is little information concerning the structure of ZnO thin films deposited by a chemical spray process based on studies by transmission electron microscopy, this might help to give a better understanding of the growth process and the effects of the intentionally added impurities.

Conclusions

The doping of ZnO thin films with, either anionic or cationic impurities using the chemical spray technique influences the electrical behavior of the as-deposited films. For similar deposition conditions the type of impurity used determines the particular characteristics of the electrical and morphological properties. From HREM micrographs for all the doped ZnO films reported in this study, besides the polycrystalline configuration detected from diffraction studies we can conclude that, the films deposited by spray pyrolysis have grown after coalescence of very small nanostructured grains.

Acknowledgments

The authors acknowledge to A. Flores, C. Magaña, M. A. Luna-arias, and L. Rendón (IF-UNAM) for their contributions. Dwight R. Acosta acknowledges the financial

support from the CONACyT (México) through a project grant number 49536.

References

1. S. Major and K.L. Chopra, *Sol. Energy Mater.* 17 (1988) 319-327.
2. M.A. Martinez, J. Herrero and M.T. Gutierrez, *Sol. Energy Mater. Sol. Cells* 45 (1997) 75-86.
3. K. Beighit, M.A. Subhan, U. Rülhe, S. Duchemin and J. Bougnot, *Proceedings of the 10th European Photovoltaic Solar Energy Conference, Lisbon Portugal, April 8-12 (1991)* 613-615.
4. G. Ferblantier, F. Maily, R. Al Asmar, A. Foucaran and F. Pascal-Delannoy, *Sens. Actuators, A* 122 (2005) 184-188.
5. M. Labeau, P. Rey, J.L. Deschanvres, J.C. Joubert and G. Delabouglise, *Thin Solid Films*, 213 (1992) 94-98.
6. M. Shinoda, T. Nishide, Y. Sawada, M. Hosaka and T. Matsumoto, *Jpn. J. Appl. Phys., Part 2* 32(1993) L1565.
7. M. Wei, D. Zhi and J.L. MacManus-Driscoll, *Scr. Mater.* 54 (2006) 817-821.
8. C. Leach and K. Vernon-Parry, *J. of Mater. Sci.* 41 (2006) 3815-381.
9. J. Ebothe, A. El Hichou, P. Vautrot and M. Addou, *J. Appl. Phys.* 93 (2003) 632-640.
10. L. Castañeda, O.G. Morales-Saavedra, J.C. Cheang-Wong, D.R. Acosta, J.G. Bañuelos, A. Maldonado and M. de la L. Olvera, *J. Phys.: Condens. Matter* 18 (2006) 5105-5120.
11. H. Gómez, A. Maldonado, M. de la L. Olvera and D.R. Acosta, *Sol. Energy Mater. Sol. Cells* 87(2005) 107-116.
12. M. de la L. Olvera, A. Maldonado, R. Asomoza, O. Solorza and D.R. Acosta, *Thin Solid Films* 394 (2001) 242-249.
13. A. Guillén-Santiago, M. de la L. Olvera, A. Maldonado, R. Asomoza and D.R. Acosta, *Phys. Status Solidi A* 201 (2004) 952-959.